Comparative Assessment of Shell Properties in Eight Species of Cohabiting Unionid Bivalves

Authors: Prezant, Robert S., Dickinson, Gary H., Chapman, Eric J., Mugno, Raymond, Rosen, Miranda N., et al.

Source: Freshwater Mollusk Biology and Conservation, 25(1) : 27-36

Published By: Freshwater Mollusk Conservation Society

URL: https://doi.org/10.31931/FMBC-D-21-00001

Freshwater Mollusk Biology and Conservation 25:27–36, 2022

DOI:10.31931/FMBC-D-21-00001

REGULAR ARTICLE

COMPARATIVE ASSESSMENT OF SHELL PROPERTIES IN EIGHT SPECIES OF COHABITING UNIONID BIVALVES

Robert S. Prezant[1]*, Gary H. Dickinson[2], Eric J. Chapman[3], Raymond Mugno[4], Miranda N. Rosen[2], and Maxx B. Cadmus[2]

[1] *Academic Affairs, Southern Connecticut State University, New Haven, CT 06515 USA*
[2] *Department of Biology, The College of New Jersey, Ewing, NJ 08628-0718 USA*
[3] *Western Pennsylvania Conservancy, Watershed Conservation Program, Indiana, PA 15701 USA*
[4] *Department of Mathematics, Southern Connecticut State University, New Haven, CT 06515 USA*

ABSTRACT

Freshwater unionid mussels produce a bilayered shell with the mineral proportion comprising an outer prismatic and an inner nacreous layer. The shell is the animals' primary structural means of protection from predators and environmental challenges; therefore, variations in shell strength and properties may lead to differences in survival. Few studies have systematically assessed shell properties in unionids. A major challenge in such work is separating effects of environment from those of evolutionary history, because ultimately, both can affect shell properties. We collected eight species of unionids within a small area of the Allegheny River, Pennsylvania, that was relatively homogeneous in substratum type and other environmental characteristics. For each species, we quantified shell thickness, including thickness of the prismatic and nacreous layers, and shell micromechanical properties (microhardness and crack propagation, a measure of fracture resistance) in three regions of the shell. Shell thickness varied dramatically among species and was about five times greater in the thickest-shelled species, *Pleurobema sintoxia*, than in the thinnest-shelled species, *Villosa iris*. Because all species experienced similar environmental conditions, variation in shell thickness can be attributed largely to evolutionary history. In contrast, microhardness and crack propagation showed little variation among species. Given that micromechanical properties are similar among species, shell strength may be largely a function of thickness. These results have conservation implications, as differences in shell thickness could reflect relative vulnerability to predators and physical conditions.

KEY WORDS: Unionidae, shell biomechanics, shell strength, nacre, prismatic

INTRODUCTION

Bivalve mollusks possess a multilayered shell, which serves to protect the animal from predators and hydrodynamic forces. In freshwater unionacean bivalves, the mineralized portion of the shell regularly consists of an outer prismatic layer and an inner nacreous layer (Checa and Rodriguez-Navarro 2001). This prismato-nacreous shell represents the most primitive of the extant bivalve shell structures (Giribet and Wheeler 2002; Graf and Cummings 2006; Marin et al. 2008). The role of the environment and local habitat in modifying the macro- and microstructure of shells has been well documented (e.g., Tan Tiu and Prezant 1987, 1989; Bailey and Green 1988; Prezant et al. 1988; Zieritz et al. 2010; Kishida and Sasaki 2018). In the field, however, environmental conditions often covary with local species composition, making it difficult to separate the effect of environment from that of evolutionary history in the development of shell properties.

Variations in shell properties can influence the strength of a shell and its resistance to fracture. The correlation between shell size, including shell thickness, and vulnerability to predation has been documented (Tyrrell and Hornbach 1998; Edelman et al. 2015). Shell strength is essentially resistance to breakage; shell fracture resistance is a measure of how easily a shell responds to an initial impact—that is, how easily a

*Corresponding Author: prezantr1@southernct.edu

fracture propagates through a shell. Variables that can affect shell strength include overall size, mass, shape, and sculpture; shell thickness and the thickness of composite layers; shell microstructural type and the nanometer and micrometer-scale mechanical properties of these microstructures; elemental content; and organic content, including intracrystalline organics (Fratzl et al. 2007; Meyers and Chen 2014; Kim et al. 2016). Shell microstructure and associated organic matrix are essential in resisting fractures from an incipient crack, for example, from a crayfish or other predator, by dissipating that initial fracture through organic interstices between calcified units without compromising the integrity of the entire mineralized shell (Zhang et al. 2019).

For unionids, studies that systematically assess structural and mechanical properties in multiple species from the same geographic location are rare. The opportunity to compare eight sympatric species of freshwater mussels availed itself through an initiative to translocate large numbers of unionids from beneath the Hunter Station Bridge (SR 62) over the Allegheny River in northwestern Pennsylvania during bridge replacement. We were able to obtain specimens from common species to assess shell properties. Our goal was to quantify shell size and thickness (including that of the nacreous vs. prismatic layers), microhardness (a measure of resistance to mechanical deformation that scales with shell strength) and fracture resistance across a variety of unionid taxa all from the same habitat, thus eliminating variation due to major differences in environment. From a conservation perspective, assessing variation in shell-layer thickness, shell strength, and fracture resistance can provide insight on survivability of unionids in the face of predatory pressures and changing environments.

MATERIALS AND METHODS

Collection Methodology

All mussels collected for this project were removed from the direct impact zone of the Hunter Station Bridge replacement, which occurred in summer 2016. The bridge is located on the Allegheny River in the town of Hunter, Pennsylvania, at 41°31′N 79°29′W. The river is relatively shallow (<3.0 m) in this area and flows are dependent upon releases from the Kinzua Dam on the Allegheny River and Tionesta Dam on Tionesta Creek.

Divers collected freshwater mussels in August 2016 using scuba, surface-supplied air, or snorkel gear depending upon river depth and current velocity. We mapped the entire survey reach of 4,884 m^2 and overlaid it with a grid for salvage purposes. We collected, enumerated, and bagged by species all mussels found within each of the salvage cells. This was not a survey study per se but a bulk translocation effort to better ensure survival of rare and endangered species of unionids. Thus, aside from anecdotal notes, specific details for quadrats or individual organisms collected are not available. We randomly selected individuals from among those recovered and held them in mesh bags in the Allegheny River until approximately 10 individuals per species were recovered. We analyzed eight species, including *Actinonaias ligamentina, Eurynia dilatata*, *Lampsilis ovata*, *Lampsilis fasciola*, *Pleurobema sintoxia*, *Ptychobranchus fasciolaris*, *Strophitus undulatus*, and *Villosa iris*.

The substratum was similar across the entire sampled reach of the river and was dominated by cobble (40%) and gravel (30%), with some sand (15%), silt (10%), and boulders (5%) present. The distribution of the eight species within this study was homogeneous across the sampled area. No obvious microhabitats were detected that might have created distribution bias for any one species. Most cells surveyed had some eelgrass (*Vallisenaria americana*) present; there are suggestions that survey cells with denser populations of eelgrass tended to have higher numbers of mussels but no differences in species diversity. The eight species assessed in this study were found in all survey cells, and their distribution (as opposed to the total numbers of unionids found) did not appear to vary with presence or absence of eelgrass or eelgrass density.

Sample Preparation

Mussels were preserved in 70% ethanol for shell analyses. While preservation in ethanol followed by drying can potentially influence shell mechanical properties (Leung and Sinha 2009; Brown et al. 2017), it is unlikely that these factors would differ among species or treatment groups. Since shells used in this study were uniformly preserved in 70% ethanol, and testing conditions were identical for all species, any alterations of the prismato-nacreous shell properties due to preservation and sample preparation should be uniform across species.

We used left shell valves for all assessments, with five valves randomly selected per species. Individual valves were removed from ethanol and any adhering soft tissue removed using a scalpel. Prior to cutting each sample, a line was drawn perpendicular to shell growth ridges, from the umbo to the growth edge of the shell (Fig. 1A). Samples were cut along this line using a water-cooled diamond band saw (model C-40, Gryphon Corporation, Sylmar, CA, USA). This produced two portions of the valve; the anterior portion was used for curved height measurements (see below), while the posterior portion was cut further and embedded for mechanical and thickness testing. Specifically, on the posterior portion of the shell, a second cut was made parallel to, and approximately 0.5–1.0 cm further posterior to, the first. The strip of shell produced from these cuts was then cut perpendicular to the original cuts into three equal-size segments, denoted as regions 1 (umbonal), 2 (midvalve), and 3 (periphery) (Fig. 1A). Shell segments were washed with distilled water after cutting, then dried at room temperature overnight, and finally dried at 45°C under 27 mm Hg in a vacuum oven for 24 h.

Shell segments were embedded in epoxy resin to enable polishing. We placed the dry shell segments individually into 31.75-mm mounting cups with the anterior side of the segment

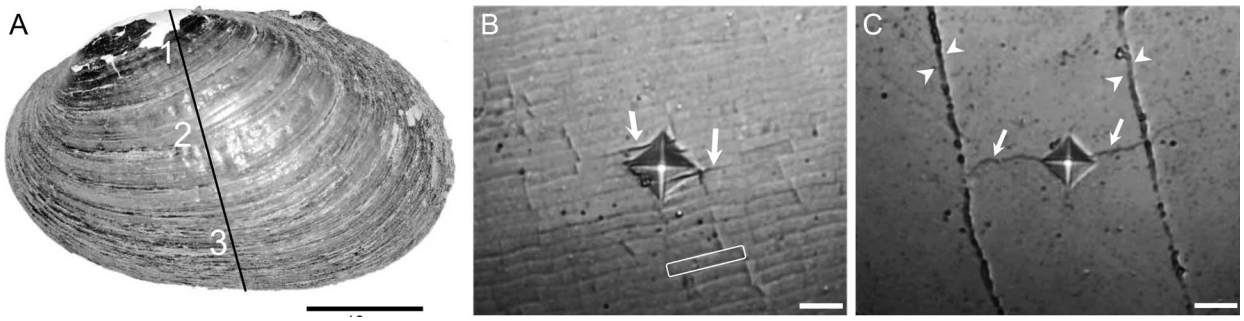

Figure 1. (A) *Actinonaias ligamentina*, left valve, showing regions of shell sampling for microhardness, crack propagation, and thickness measurements. Region 1 is umbonal, region 2 is midvalve, and region 3 is shell periphery. Light microscopy images of an indent (diamond shape) made within (B) the nacre and (C) the prismatic layer. An applied load of 30 g was used during indentation in both shell regions. Tailed arrows indicate cracks produced during indentation. (B) Individual nacre tablets are clearly designated as noted by the white rectangle. For the prismatic layer, the boundary between adjacent units is indicated by arrowheads. Scale bars: A = 10 mm; B and C = 5 μm.

oriented facing the bottom of the mounting cup. Samples that did not stand upright on their own were secured using plastic coil clips (Allied High Tech, Compton, CA, USA). Mounting cups were filled with epoxy (EpoxySet, Allied High Tech) and cured for approximately 24 h or until completely hardened.

Samples were polished using an automated grinder polisher machine (METPREP 3 PH-4, Allied High Tech). Each embedded sample was polished through a series of 320-grit, 600-grit, and 800-grit silicon carbide papers, then polished with a 1-μm polycrystalline diamond suspension and lastly a 0.04-μm colloidal silica suspension. Samples were cleaned between each polishing step with a solution of 2% microorganic soap. Once the polished surface was completely smooth and free of scratches, samples were dried at room temperature and then placed in a desiccator until testing.

Shell Curved-Height Measurements

The anterior portion of the shell valve produced after the initial cut (see above) was used for curved-height measurements. Images of the cut surface of each valve were scanned using a photo scanner to enable digital measurements. This was done by placing the cut surface of the valve directly onto the bed of the scanner so that the shell stood up on its own, and a high-resolution scan was acquired. Curved height, defined as the total distance from umbo to the ventral growth edge, was measured in ImageJ (Ver. 1.43, U.S. National Institutes of Health, Bethesda, Maryland, USA, https://imagej.nih.gov/ij/, accessed February 15, 2022) on the scans using a segmented line tool. To incorporate curvature of the valve, the line was drawn down the center of the cut surface of the valve from umbo to the shell edge.

Shell Thickness Measurements

We assembled panorama images of each embedded shell sample using Zen 2.3 software (Carl Zeiss Microscopy, White Plains, NY, USA). Individual images were taken under brightfield using an Axioscope A1 reflected-light microscope with an Axiocam 105 color camera (Carl Zeiss Microscopy). The number of individual images varied depending on the size of the sample and ranged from 3 to 36. We measured shell thickness at defined points along the breadth of each embedded shell segment. Measurement locations were determined by placing a grid over the image as described in Nardone et al. (2018). Thickness measurements were taken using the software's linear measurement tool for the prismatic and nacreous layers. Grid sizes varied depending on the size of the sample but were adjusted to enable 20–30 measurements per sample. In the samples that were from the region closest to the umbo (region 1), erosion produced a prismatic layer that was often not continuous, and in some cases, was missing completely, and therefore measurements were not recorded for this layer. In samples that contained the growth edge, measurements were recorded until the layers began to thin. Measurements from the nacreous and prismatic layers were added together to determine the total thickness. For regions containing a prismatic layer (regions 2 and 3), the ratio of prismatic to nacreous thickness was calculated as the prismatic layer thickness divided by the nacreous layer thickness.

Micromechanical Testing

Micromechanical testing was conducted on an HM-200 microhardness testing machine (Mitutoyo America Corporation, Aurora, IL, USA) on five individuals per species per shell region. Embedding and polishing of shell segments produced a cross-section of the shell, normal to the outer shell surface, as described in Dickinson et al. (2012). This procedure enabled separate tests to be made within both the prismatic and nacreous layers (Fig. 1B, C). In each sample, 10 indents were made in both the prismatic and nacreous layers. Values obtained from these repeated indentations were averaged for each shell layer prior to statistical analyses. Indents were spaced evenly along the breadth of the shell segment using the stage-positioning micrometers on the testing machine, with spacing between indents equivalent in the prismatic and

nacreous layers. Micromechanical indents were made at 30 g load and 5 s dwell time within both the prismatic and nacreous layers. For the first two replicates from each species, indents were measured directly on the hardness tester in two dimensions and Vickers hardness numbers (VHNs) were automatically calculated by the tester. For the other three replicates from each species, an image of each indent was taken using a Zeiss Axiocam 305 color microscope camera and the diagonals of the indent were measured on the digital image using Zen 2.3 software (Carl Zeiss Microscopy). We used the equation $1.854 \times F/d^2$ where F is force in kilograms and d^2 is the mean diagonal length in millimeters to calculate microhardness as a VHN (ASTM 2017). Variation between the two measurement techniques was minimal (on average, within 2.5% when the same indent was measured both ways). In samples from the region closest to the umbo (region 1 as shown in Fig. 1A), the prismatic layer was not continuous (due to umbonal erosion) and therefore microhardness could not be measured in the prismatic layer for these samples.

For all sample sets, crack propagation was assessed on digital microscope images taken on the hardness tester (Fig. 1B, C). Crack propagation was determined as the radius of a circle emanating from the center of the indent and encompassing all visible cracks (Anstis et al. 1981; Baldassarri et al. 2008).

Statistical Analyses

We explored differences in the response variables of measured hardness, crack propagation, curved height, and thickness among species. Since measured hardness, crack propagation, and thickness values were consistently and substantially different between the nacreous and prismatic layers (for example, by up to an order of magnitude for thickness metrics), these layers were analyzed separately. All response variables failed to satisfy the assumptions of analysis of variance, using either the Levene's test for homogeneity of variance or the Shapiro–Wilk test for normality, so we used nonparametric methods that compare median values (Ott and Longnecker 2010). The overall significance level was set at $P < 0.05$. Statistical tests were conducted in R (R Core Team 2013). We compared curved height among species using a Kruskal–Wallis test and Dunn's procedure for multiple comparisons with Holm's correction for P values (Pohlert 2014). We assessed the effect of species on shell microhardness and crack propagation using the Prentice test, which is a generalization of Friedman's test for use with replicates (Konietschke et al. 2015). Shell region was used as a blocking variable. Using Tukey's method, we made multiple comparisons between individual species. For thickness and the prismatic:nacreous-layer ratio, a Prentice test was also used, but multiple comparisons were made using pairwise Wilcoxon rank sum tests. This was due to missing values (shell samples where the nacre or prismatic layer was fractured and therefore thickness could not be measured) causing errors when using the Tukey's method (R Core Team 2013).

RESULTS

Visual examination of shell valves used from the eight species revealed an obvious difference in overall size of the shells, as well as variation in relative thickness of prismatic and nacreous layers; quantification of curved height and shell thickness support these observations. Curved height varied significantly among species (Kruskal–Wallis test: $H = 32.119$, $df = 7$, $P < 0.0001$; Fig. 2A). Curved height was nearly 2.5 times greater in the largest species tested, *L. ovata,* as compared to the smallest, *V. iris* (Dunn's multiple comparisons with Holm's correction: $P < 0.05$). Likewise, thickness of both the nacreous layer (Prentice test: $T = 90.305$, $df = 7$, $P < 0.0001$; Fig. 2B) and prismatic layer (Prentice test: $TS = 60.459$, $df = 7$, $P < 0.0001$; Fig. 2C) differed significantly among species. Nacre thickness was about eight times greater in the thickest species, *P. sintoxia,* as compared to the thinnest, *V. iris* (Wilcox rank sum tests: $P < 0.05$). *Lampsilis fasciola* had the thickest prismatic layer, with thickness about four times greater than *V. iris* (Wilcox rank sum tests: $P < 0.05$). For curved height and thickness metrics, numerous significant pairwise differences were observed between species, as detailed in Figure 2. Among all species and all shell regions, average nacreous layer thickness was about five times greater than that of the prismatic layer (note the difference in y-axis scale between Fig. 2B and C).

When comparing among regions of each shell valve (see Fig. 1), nacreous layer thickness for all species tended to be greatest closer to the umbo (region 1), reflecting the older age and longer mineral deposition times (Fig. 2B). The thinnest nacreous layer was typically found in region 3, nearest the valve edge, which is the youngest part of the shell with the shortest deposition time. Nacre was present in each region 3 measured, confirming that samples from these areas were always internal to the pallial line and not at the most distal shell margin.

As the outer layer of calcified shell, the prismatic layer is also most susceptible to external erosive conditions once the periostracum is either worn away or dissolved (not uncommon in unionids). As such, in the specimens collected, the umbonal area of prismatic shell (region 1) was consistently eroded and we were unable to take representative measurements of prismatic thickness. The shell periphery (region 3) in all taxa had the thickest prismatic layer (Fig. 2C).

The prismatic:nacreous-layer ratio varied significantly among species (Prentice test: $T = 52.684$, $df = 7$, $P < 0.0001$; Fig. 2D). Of note, this ratio was significantly lower in *P. sintoxia* compared to each of the other species assessed (Wilcox rank sum tests: $P < 0.05$); thus, nacre comprised a greater proportion of the total shell in this species (Table 1). The prismatic:nacreous-layer ratio did not differ significantly among any of the other species tested, except between *E. dilatata* and *L. ovata* (Wilcox rank sum tests: $P < 0.05$). Nacre comprised the bulk of total shell thickness in nearly all samples (with one exception, *L. fasciola*, region 3), as evidenced by prismatic:nacre ratios consistently well below 1.

Despite variations in nacreous thickness among species,

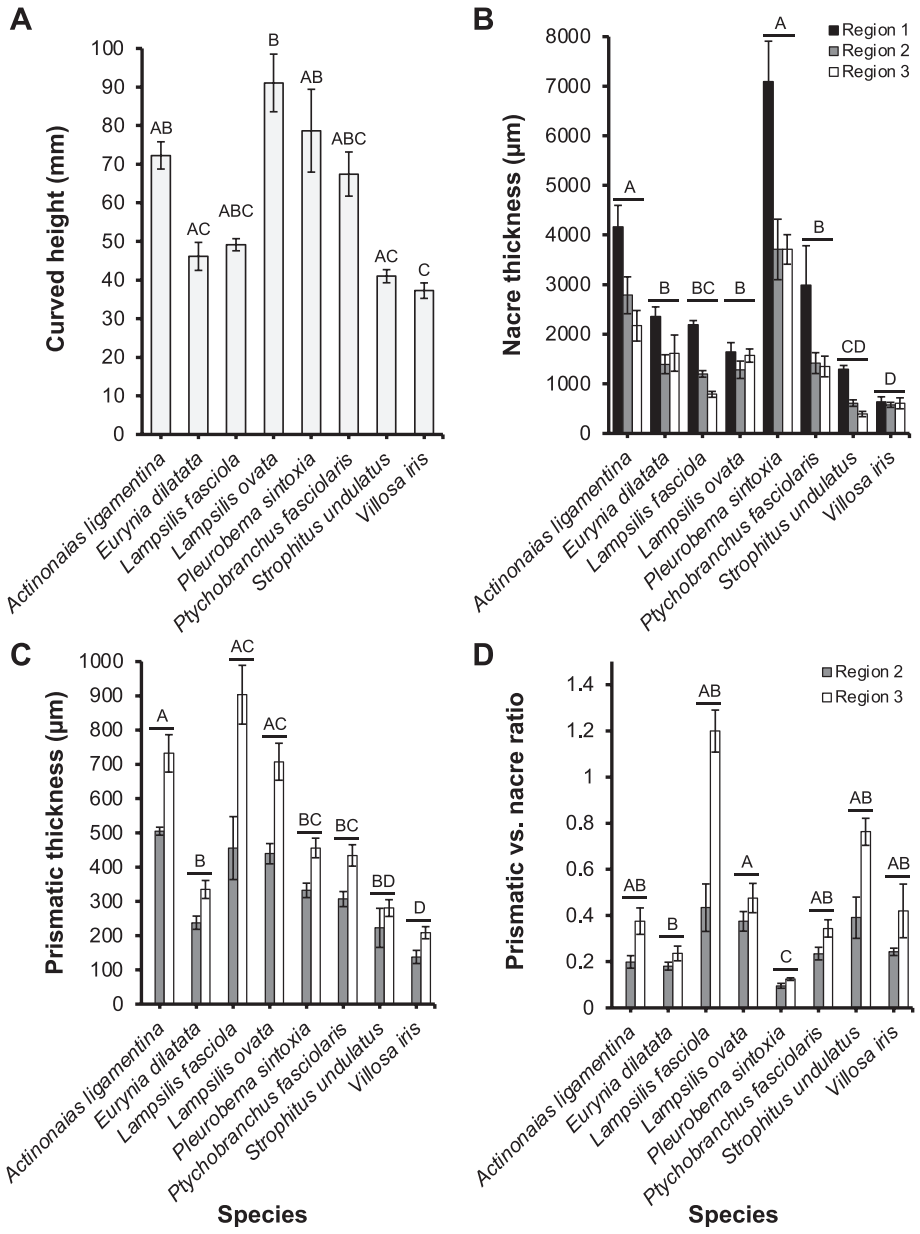

Figure 2. Curved height and thickness metrics (mean ± SE). (A) Curved height of left shell valves. (B) Nacre layer thickness. (C) Prismatic layer thickness. (D) Prismatic:nacrelayer thickness ratio. Within each panel, species marked with different letters are significantly different from one another, whereas those that share a letter do not differ. For curved height, pairwise comparisons were made using Dunn's multiple comparisons with Holm's correction ($P < 0.05$). For all other metrics, pairwise comparisons were made using Wilcoxon rank sum tests ($P < 0.05$), with region grouped within species. $n = 5$ replicates per species per shell region.

there was no effect of species on nacre microhardness (Prentice test: $T = 7.328$, df $= 7$, $P = 0.393$; Fig. 3A). Across all taxa and all shell regions measured, values ranged from 198 to 271 VHN. As with nacre, differences in microhardness in the prismatic layers among the species were minimal. Although the overall effect of species on microhardness was significant (Prentice test: $T = 18.21$, df $= 7$, $P = 0.011$; Fig. 3B), the only pairwise difference among the species assessed was between *L. ovata* and *E. dilatata* (Tukey's method: $P < 0.05$). Across all taxa and all shell regions measured, prismatic microhardness ranged from 258 to 419 VHN. For all species and all shell regions, the prismatic layer was consistently harder (on average, by 54%) than the nacre.

Higher crack propagation implies a lower resistance to the growth of fractures through a particular shell layer. There was relatively little difference across taxa in crack propagation resistance, nor was there much variation in resistance dependent upon shell location (Fig. 3C, D). There was a significant effect of species within the nacre (Prentice test: $T = 22.378$, df $= 7$, $P = 0.002$; Fig. 3A). However, significant

Table 1. Shell valve thickness metrics. Values are mean ± SE; $n = 5$ replicates per species per shell region. Region 2 = midvalve; region 3 = shell periphery.

	AL	ED	LF	LO	PS	PF	SU	VI
Region 2								
Total thickness (mm)	3.29 ± 0.38	1.62 ± 0.21	1.70 ± 0.11	1.72 ± 0.20	4.05 ± 0.63	1.73 ± 0.23	0.84 ± 0.08	0.71 ± 0.07
% thickness as prismatic	16.1 ± 1.8	15.1 ± 1.1	25.9 ± 4.5	26.2 ± 2.3	8.7 ± 0.9	18.4 ± 1.4	25.8 ± 4.5	19.2 ± 1.3
% thickness as nacre	83.9 ± 1.8	85.5 ± 1.4	71.2 ± 3.0	74.0 ± 2.1	91.1 ± 0.8	81.0 ± 1.9	72.7 ± 4.9	81.1 ± 1.2
Region 3								
Total thickness (mm)	2.90 ± 0.34	1.95 ± 0.39	1.70 ± 0.13	2.27 ± 0.13	4.17 ± 0.32	1.78 ± 0.23	0.67 ± 0.08	0.82 ± 0.12
% thickness as prismatic	26.1 ± 2.8	18.9 ± 2.1	53.0 ± 2.0	31.6 ± 3.2	11.0 ± 0.4	25.4 ± 2.2	42.4 ± 1.7	27.7 ± 4.7
% thickness as nacre	73.9 ± 2.8	81.1 ± 2.1	46.6 ± 2.2	68.6 ± 3.0	89.0 ± 0.4	74.5 ± 2.2	57.6 ± 1.7	71.9 ± 4.7

Abbreviations: AL = *Actinonaias ligamentina*; ED = *Eurynia dilatata*; LF = *Lampsilis fasciola*; LO = *Lampsilis ovata*; PS = *Pleurobema sintoxia*; PF = *Ptychobranchus fasciolaris*; SU = *Strophitus undulatus*; VI = *Villosa iris*.

pairwise differences were observed only between *P. sintoxia* and *L. ovata,* and between *P. sintoxia* and *V. iris* (Tukey's method: $P < 0.05$). Across all taxa and all shell regions measured, nacre crack propagation ranged from 8.6 μm to 18.7 μm. Variation in crack propagation within the prismatic layer among species was minimal in both regions (Fig. 3D). Overall, the effect of species was significant (Prentice test: $T = 19.760$, $df = 7$, $P = 0.006$), but individual pairwise differences between species were not significant (Tukey's method: $P > 0.05$ for all comparisons). Across all taxa and all shell regions measured, prismatic crack propagation ranged from 13.0 μm to 26.6 μm. In all species and all shell regions, crack propagation was consistently higher (on average, by 61%) in the prismatic layer as compared to the nacreous layer, suggesting that the former exhibits a lower resistance to fracture.

DISCUSSION

Shell formation in bivalve mollusks is a complex process affected by evolutionary history as well as environment (Tan Tiu and Prezant 1992; Kesler and Bailey 1993; Marin et al. 2007; Hornbach et al. 2010; Gilbert et al. 2017; Clark et al. 2020). Here, we assessed structural and mechanical properties of the shell in eight cohabiting species. Given that environmental conditions were relatively consistent among individuals—all were collected at the same location with no noticeable differences in substratum type—variation in shell properties between taxa can be attributed largely to evolutionary history. This conclusion has conservation implications, as shell structure and strength can influence population viability in the face of predation (including shell collection by humans), hydrodynamic forces, and shifts in water quality. We found that shell height and thickness varied dramatically among cohabiting species; in contrast, microscale mechanical properties were remarkably consistent among the species assessed.

At the whole-organism level, shell thickness is a good indicator of shell strength (Zuschin and Stanton 2001). Shell thickness can vary with latitude and hydrological conditions (Watson et al. 2012), as well as among species exposed to the same environment. Variation or changes in shell thickness, especially at the umbonal (oldest) areas for the latter, can leave the bivalve susceptible to shell fragmentation (Newell et al. 2007) and more vulnerable to shell-crushing predators. Unionid bivalves are preyed upon by birds, fish, a variety of mammals, crayfish, and turtles, and shell thickness and size affect predatory vulnerability (Haag 2012). In general, thinner-shelled unionids (by species or relative growth size) face greater predation threat (Leonard-Pingel and Jackson 2013). Nacre, considered the most fracture-resistant shell layer, can compose a substantive portion of total shell thickness in unionids. For the species we assessed, within the midshell region the nacreous layer comprised at least 71%, and as much as 91%, of the total shell thickness, consistent with previous assessments in *Unio elongatulus* (89% of the shell thickness, Checa 2000). Of the eight species we examined, total shell thickness in *P. sintoxia* and *A. ligamentina* (the thickest-shelled species examined) was four to six times greater than that of *S. undulatus* and *V. iris*, the species with the thinnest shells. Nacre also comprised a greater proportion of total shell thickness in *P. sintoxia*, as compared to all other species assessed. Such differences in shell thickness, and the proportion of the shell composed of fracture-resistant nacre, are likely to lead to variation in shell strength at the whole-shell level.

When considering shell thickness and relative thickness of shell layers, it must be kept in mind that nacre is usually deposited throughout the growing life of a bivalve (Marie et al. 2017). Despite the give-and-take of internal shell deposition and erosion, it is typical for nacre to thicken with age (Mann 2001). The Anodontini and Lampsilini (*Actinonais*, *Lampsilis*, *Ptychobranchus*) tend to be short-lived while the Amblimini (*Villosa*) and Pleurobemi (*Eurynia*, *Pleurobema*) are long-lived (Haag and Rypel 2011). Across the tribes examined here, one of the two species of Pleurobimini had the thickest shells in midregions, while *V. iris* (Amblemini) had the thinnest shells in middle and peripheral regions. Whether the shell thickness of *P. sintoxia* is representative of the longevity of the pleurobiminids will take additional study across more species within the group.

Despite observed differences in thickness at the micrometer scale, these bivalves, with one exception, did not show substantial variation in resistance to shell fracture or micro-

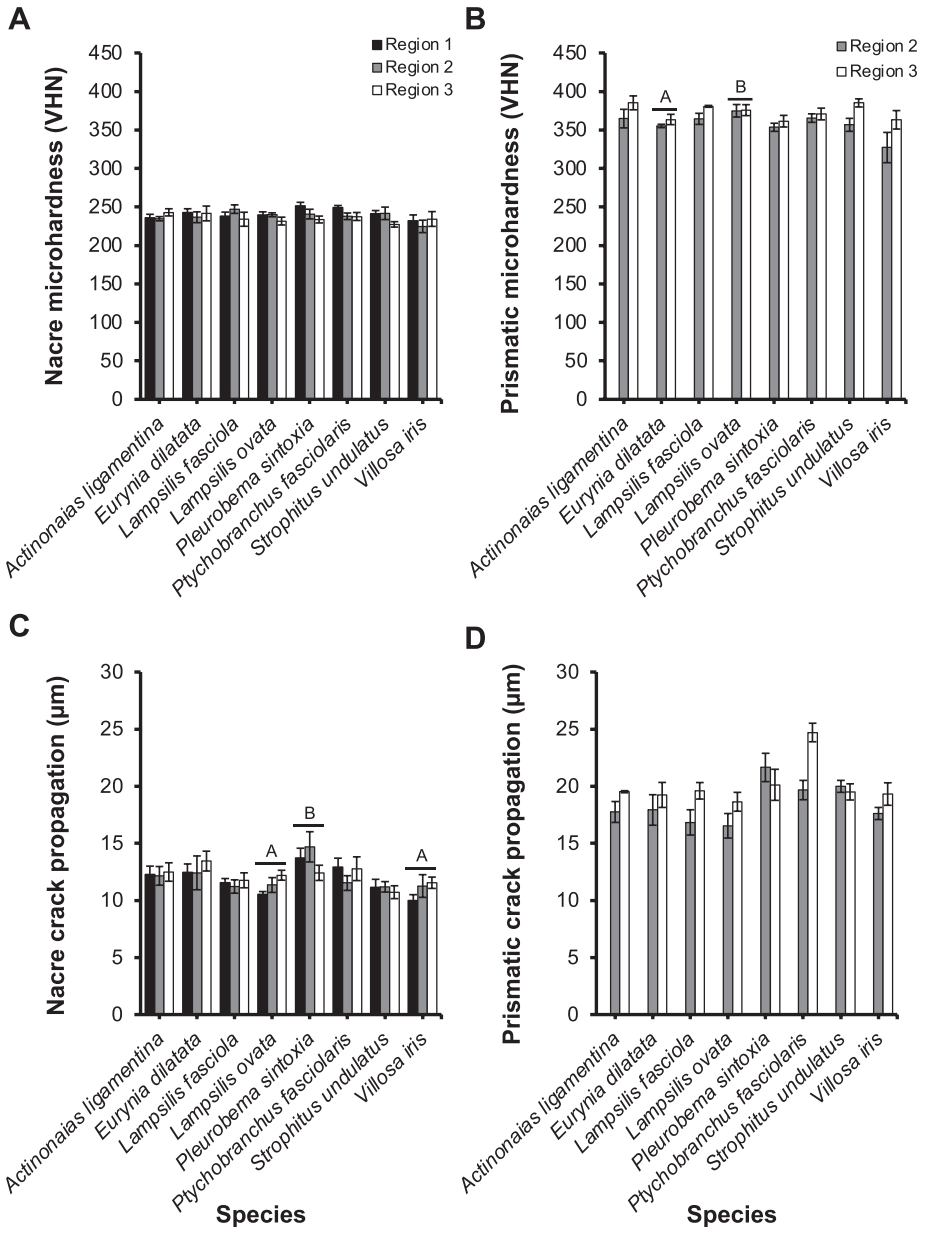

Figure 3. Micromechanical testing metrics (mean ± SE). Vickers microhardness, tested within the (A) nacre and (B) prismatic layers. Lengths of cracks propagating from indentations when tested in the (C) nacre and (D) prismatic layers. Within each panel, species marked with different letters are significantly different from one another using Tukey's method pairwise comparisons ($P < 0.05$). Species that lack a letter did not differ significantly from any of the other species assessed. $n = 5$ replicates per species per shell region.

hardness. Indeed, the thinnest-shelled unionids examined were no more vulnerable to fracture at the micrometer scale than any others we tested. The lack of correlation between nacreous layer thickness and relative fracture sensitivity is not surprising, as fractures take place at a microstructural level with fracture paths along intercrystalline junctures (Song et al. 2018). Under the load tested here, the length of cracks formed during mechanical testing (tens of micrometers) was an order of magnitude lower than nacreous layer thickness (hundreds of micrometers), even in the thinnest-shelled species (Currey 1977; Sun and Bhushan 2012). The exception noted above is *P. sintoxia,* which had the thickest nacre but showed higher crack propagation when compared to *V. iris*. The lower fracture resistance in *P. sintoxia* suggests that the nacre was tolerant of a lower fracture resistance (thus, a small crack would still have significant nacre to penetrate before the shell proper lost its structural stability). The statistical difference seen here also might be considered an outlier; overall, the difference demonstrated was small and does not impact the general trends revealed.

Molluscan shell strength reflects multiple factors, including shell thickness, shell microstructure, organic content ("con-

chiolin"), overall shape, and shell ornamentation (Zuschin and Stanton 2001). Multiple layers of different microstructures composing such shells evolved early in the lineage as demonstrated from Lower Cambrian fossils from China (Feng and Sun 2003). The multiple calcified layers offer some degree of structural plasticity because different layers differ in structural support. Nacre is resistant to fracture (Song et al. 2018), while prisms that align perpendicularly to the shell surface impart greater resistance to abrasion (Sun and Bhushan 2012). The organic interfaces that permeate the junctions between microstructures offer a path for fracture dissipation (Gim et al. 2019), while the dramatic change in structure from prismatic to nacreous structure offers a stoppage juncture. Fracture resistance in nacre reflects "constrained microcracking" (Song et al. 2018). Microcracks essentially form in advance of the primary crack deflection, releasing the local stress concentration, thus enhancing the crack extension resistance. Our data support the enhanced fracture resistance of nacre because the length of cracks produced by indentation was shorter in the nacreous layer than in the prismatic layer, implying greater fracture resistance. Microhardness showed the opposite trend, with substantially greater microhardness in the prismatic layer for all species. Similarly, the external shell layer of the large ranellid gastropod *Charonia lampas lampas* was harder than the inner layer, albeit the inner shell layer is crossed lamellar while the outer layer is prismatic (Boufala et al. 2019). It is not surprising that outer shell layers are harder than inner layers, and given the infaunal habitat of unionid mussels (and most bivalves), greater hardness of the outer (prismatic) layer enhances resistance to abrasion.

The eight unionid species assessed in this study are found typically in flowing waters, often with sand, gravel, and/or rock substratum (references noted here include information for all eight species: Burch 1975; Clarke 1981; Williams et al. 2008). The Hunter Station Bridge site is typical of their usual habitat (medium to large rivers with sand and gravel substratum). While some species of unionids are regularly found associated with specific microhabitats (Strayer 1981), there is no indication that the distribution of mussels in this study and at this site varied spatially. The consistency of habitat requirements across many unionid taxa and the uniformity of shell microhardness and fracture resistance in all mussels tested speaks to a successful and highly conservative evolutionary prismato-nacreous shell lineage. Our results suggest that shell microhardness and resistance to fracture are remarkably similar across these eight species of unionids. It also suggests that our focus, in terms of characteristics to monitor for vulnerability across unionid taxa, should not be on micrometer-scale shell strength or fracture resistance but on relative shell and shell layer (prismatic–nacreous) thicknesses.

While we uncovered a high level of conservativism in shell biomechanics within multiple species of unionids at a single location, our results suggest the need for broader study across a range of habitats to better discern environmentally induced differences in shell characters. We did not test phenotypic plasticity, but the high degree of biomechanical uniformity across these eight members of the Unionidae from two subfamilies (as per Lopes-Lima et al. 2017: Anodontinae, Ableminae) suggests that the prismato-nacreous shell of unionids has successfully supported the long-term survival of a group that dates to the Triassic (Skawina and Dzik 2011).

ACKNOWLEDGMENTS

We gratefully acknowledge the Pennsylvania Department of Transportation for allowing the retention of common mussels from the translocation project. Mussels were sacrificed by E.J.C under scientific collecting permit number 2016-01-0082 from the Pennsylvania Fish and Boat Commission. In addition, we greatly appreciate field assistance provided by Enviroscience, the United States Forest Service, and numerous Western Pennsylvania Conservancy staff members. We thank Natasha Chaudhari for collection of indentation images, and we are grateful to Rebecca Hedreen, Sciences and Distance Learning Librarian at Southern Connecticut State University, for important referencing assistance. This manuscript was improved through the contributions of the journal editors and anonymous reviewers. G.H.D and M.B.C. would like to acknowledge funding from The College of New Jersey's Mentored Undergraduate Summer Experience. M.N.R. was supported by a National Oceanic and Atmospheric Administration research grant to G.H.D. Funding to support this publication was supplied by Southern Connecticut State University.

LITERATURE CITED

Anstis, G. R., P. Chantikul, B. R. Lawn, and D. B. Marshall. 1981. A critical evaluation of indentation techniques for measuring fracture-toughness: 1, Direct crack measurements. Journal of the American Ceramic Society 64:533–538.

ASTM (American Society for Testing and Materials). 2017. ASTM Designation E384-17. Standard Test Method for Microhardness of Materials. American Society for Testing and Materials, West Conshohocken, Pennsylvania.

Bailey, R. C., and R. H. Green. 1988. Within-basin variation in the shell morphology and growth rate of a freshwater mussel. Canadian Journal of Zoology 66:1704–1708.

Baldassarri, M., H. C. Margolis, and E. Beniash. 2008. Compositional determinants of mechanical properties of enamel. Journal of Dental Research 87:645–649.

Boufala, K., S. Ouhenia, G. Louis, D. Betrancourt, D. Chicot, and I. Belabbas. 2019. Microstructure analysis and mechanical properties by instrumented indentation of *Charonia lampas lampas* shell. Journal of Mechanical Behavior of Biomedical Materials 89:114–121.

Brown, C. G., R. Fiorillo, R. Yi, S. Tangirala, and J. Ametepe. 2017. Drying, freezing, and ethanol preservation lower shell strength of two freshwater pulmonate gastropods. Georgia Journal of Science 75: 7. Available at http://digitalcommons.gaacademy.org/gjs/vol75/iss2/7 (accessed January 21, 2022).

Burch, J. B. 1975. Freshwater unionacean clams (Mollusca: Pelecypoda) of North America. Malacological Publications, Hamburg, Michigan.

Checa, A. 2000. A new model for periostracum and shell formation in Unionidae (Bivalvia, Mollusca). Tissue and Cell 32:405–416.

Checa, A.G., and A. Rodriguez-Navarro. 2001. Geometrical and crystallo-

graphic constraints determine the self-organization of shell microstructures in Unionidae (Bivalvia: Mollusca). Proceedings of the Royal Society, London 268:771–778.

Clark, M. S., L. S. Peck, J. Arivalagan, T. Backeljau, S. Berland, J. C. Cardoso, C. Caurcel, G. Chapelle, M. De Noia, S. Dupont, K. Gharbi, J. I. Hoffman, K. S. Last, A. Marie, F. Melzner, K. Michalek, J. Morris, D. M. Power, K. Ramesh, T. Sanders, K. Sillanpää, V. A. Sleight, P. J. Stewart-Sinclair, K. Sundell, L. Telesca, D. L. J. Vendrami, A. Ventura, T. A. Wilding, T. Yarra, and E. M. Harper. 2020. Deciphering mollusc shell production: the roles of genetic mechanisms through to ecology, aquaculture and biomimetics. Biological Reviews 95:1812–1837.

Clarke, A. H. 1981. The Freshwater Molluscs of Canada. National Museum of Natural Sciences, National Museums of Canada, Ottawa.

Currey, J. D. 1977. Mechanical properties of mother of pearl in tension. Proceedings of the Royal Society of London. Series B. Biological Sciences 196:443–463.

Dickinson, G. H., A. V. Ivanina, O. B. Matoo, H. O. Portner, G. Lannig, C. Bock, E. Beniash, and I. M. Sokolova. 2012. Interactive effects of salinity and elevated CO_2 levels on juvenile eastern oysters, *Crassostrea virginica*. Journal of Experimental Biology 215:29–43.

Edelman, A. J., J. Moran, T. J. Garrabrant, and K. C. Vorreiter. 2015. Muskrat predation of native freshwater mussels in Shoal Creek, Alabama. Southeastern Naturalist 14: 473–483.

Feng, W., and W. Sun. 2003. Phosphate replicated and replaced microstructure of molluscan shells from the earliest Cambrian of China. Acta Palaeontologica Polonica 48:21–30.

Fratzl, P., H. S. Gupta, F. D. Fischer, and O. Kolednik. 2007. Hindered crack propagation in materials with periodically varying Young's modulus—Lessons from biological materials. Advanced Materials 19:2657–2661.

Gilbert, P. U. P. A., K. D. Bergmann, C. E. Myers, M. A. Marcus, R. T. Devol, C.-Y. Sun, A. Z. Blonsky, E. Tamre, J. Zhao, E. A. Karan, N. Tamura, S. Lerner, A. J. Giuffre, G. Giribet, J. M. Eiler, and A. H. Knoll. 2017. Nacre tablet thickness records formation temperature in modern and fossil shells. Earth and Planetary Science Letters 460:281–292.

Gim, J., N. Schnitzer, L. M. Otter, Y. Cui, S. Motreuil, F. Marin, S. E. Wolf, D. E. Jacob, A. Misra, and R. Hovden. 2019. Nanoscale deformation mechanics reveal resilience in nacre of *Pinna nobilis* shell. Nature Communications 10:1–8.

Giribet, G., and W. Wheeler. 2002. On bivalve phylogeny: A high-level analysis of the Bivalvia (Mollusca) based on combined morphology and DNA sequence data. Invertebrate Biology 121:271–324.

Graf, D. L., and K. S. Cummings. 2006. Palaeoheterodont diversity (Mollusca: Trigonoida + Unionoida): What we know and what we wish we knew about freshwater mussel evolution. Zoological Journal of the Linnean Society 148:343–394.

Haag, W. R. 2012. North American Freshwater Mussels. Cambridge University Press, New York.

Haag, W. R., and A. L. Rypel. 2011. Growth and longevity in freshwater mussels: Evolutionary and conservation implications. Biological Reviews 86:225–247.

Hornbach, D. J., V. J. Kurth, and M. C. Hove. 2010. Variation in freshwater mussel shell sculpture and shape along a river gradient. American Midland Naturalist 164:22–36.

Kesler, D. H., and R. C. Bailey. 1993. Density and ecomorphology of a freshwater mussel (*Elliptio complanata*, Bivalvia: Unionidae) in a Rhode Island Lake. Journal of the North American Benthological Association 12:259–264.

Kim, Y.-Y., J. D. Carloni, B. Demarchi, D. Sparks, D. G. Reid, M. E. Kunitake, C. C. Tang, M. J. Duer, C. L. Freeman, and B. Pokroy. 2016. Tuning hardness in calcite by incorporation of amino acids. Nature Materials 15:903.

Kishida, K., and T. Sasaki. 2018. Geographical and seasonal variations of the shell microstructures in the bivalve *Scapharca broughtonii*. Pages 177–186 *in* K. Endo, T. Kogure, and H. Nagasawa, editors. Biomineralization: From Molecular and Non-Structural Analyses to Environmental Science. Springer, Singapore.

Konietschke, F., M. Placzek, F. Schaarschmidt, and L. A. Hothorn. 2015. nparcomp: An R software package for nonparametric multiple comparisons and simultaneous confidence intervals. Journal of Statistical Software 64:1–17.

Leonard-Pingel, J. S., and J. B. C. Jackson. 2013. Drilling intensity among Neogene tropical Bivalvia in relation to shell forms and life habit. Bulletin of Marine Science 89:905–919.

Leung, H. M., and S. K. Sinha. 2009. Scratch and indentation tests on seashells. Tribology International 42:40–49.

Lopes-Lima, M., E. Froufe, V. T. Do, M. Ghamizi, K. E. Mock, U. Kebapci, O. Klishko, S. Kovitvadhi, U. Kovitvadhi, O. S. Paul, J. M. Pfeiffer 3rd, M. Raley, N. Riccardi, H. Sereflisan, R. Sousa, A. Teixeira, S. Varandas, X. P. Wu, D. T. Zanatta, A. Zieritz, and A. E. Bogan. 2017. Phylogeny of the most species-rich freshwater bivalve family (Bivalvia: Unionida: Unionidae): Defining modern subfamilies and tribes. Molecular Phylogeny and Evolution 106:174–191.

Mann, S. 2001. Biomineralization: Principles and Concepts in Bioinorganic Materials Chemistry. Oxford University Press, New York.

Marie, B., J. Arivalagna, L. Marthéron, G. Bolbach, S. Berland, A. Marie, and F. Marin. 2017. Deep conservation of bivalve nacre proteins highlighted by shell matrix proteomics of the Unionoida *Elliptio complanata* and *Villosa lienosa*. Journal of the Royal Society Interface 14:20160846.

Marin, F., G. Luquet, B. Marie, and D. Medakovic. 2008. Molluscan shell proteins: primary structure, origin, and evolution. Current Topics in Developmental Biology 80: 209–276.

Meyers, M. A., and P. Chen. 2014. Biological Materials Science: Biological Materials, Bioinspired Materials, and Biomaterials. Cambridge University Press, Cambridge. United Kingdom.

Nardone, J. A., S. Patel, K. R. Siegel, D. Tedesco, C. G. McNicholl, J. O'Malley, J. Herrick, R. A. Metzler, B. Orihuela, D. Rittschof, and G. H. Dickinson. 2018. Assessing the impacts of ocean acidification on adhesion and shell formation in the barnacle *Amphibalanus amphitrite*. Frontiers in Marine Science 5:369.

Newell, A. J., D. J. Gower, M. J. Benton, and V. P. Tverdokhlebov. 2007. Bedload abrasion and the *in-situ* fragmentation of bivalve shells. Sedimentology 54:835–845.

Ott, L. O., and M. Longnecker. 2010. An Introduction to Statistical Methods and Data Analysis. Brooks/Cole, Cengage Learning, Belmont, California.

Pohlert, T. 2014. The Pairwise multiple comparison of mean ranks package (PMCMR). R package. Available at http://CRAN.R-project.org/package=PMCMR (accessed January 21, 2022).

Prezant, R. S., A. Tan Tiu, and K. Chalermwat. 1988. Shell microstructure and color changes in stressed *Corbicula fluminea* (Bivalvia: Corbiculidae). The Veliger 31:236–243.

R Core Team. 2013. R: A language and environment for statistical computing. R Foundation for Statistical Computing, Vienna, Austria. Available at http://www.R-project.org/ (accessed January 21, 2022).

Skawina, A., and J. Dzik. 2011. Umbonal musculature and relationships of the Late Triassic filibranch unionid bivalves. Zoological Journal of the Linnaean Society 163:863–883.

Song, J., Fan, C., H. Ma, L. Liang, and Y. Wei. 2018. Crack deflection occurs by constrained microcracking in nacre. Acta Mechanica Sinica 34:143–150.

Strayer, D. 1981. Notes on the microhabitats of Unionid mussels in some Michigan streams. American Midland Naturalist 106:411–415.

Sun, J., and B. Bhushan. 2012. Hierarchical structure and mechanical properties of nacre: A review. RSC Advances 2:7617–7632.

Tan Tiu, A., and R. S. Prezant. 1987. Shell microstructural responses of *Geukensia demissa granosissima* (Mollusca, Bivalvia) to continual submergence. American Malacological Bulletin 5:173–176.

Tan Tiu, A., and R. S. Prezant. 1989. Temporal variation in microstructure of the inner shell surface of *Corbicula fluminea* (Bivalvia: Heterodonta). American Malacological Bulletin 7:65–71.

Tan Tiu, A., and R. S. Prezant. 1992. The role of environment in shell growth dynamics of the Asian clam *Corbicula fluminea* (Mollusca: Bivalvia). Malacological Review 25:109–117.

Tyrrell, M., and D. J. Hornbach. 1998. Selective predation by muskrats on freshwater mussels in 2 Minnesota rivers. Journal of the North American Benthological Society 17:301–310.

Watson, S. A., L. S. Peck, P. A. Tyler, P. C. Southgate, K. S. Tan, R. W. Day, and S. A. Morley. 2012. Marine invertebrate skeleton size varies with latitude, temperature and carbonate saturation: implications for global change and ocean acidification. Global Change Biology 18:3026–3038.

Williams, J. D., A. E. Bogan, and J. T. Garner. 2008. Freshwater mussels of Alabama and the Mobile Basin in Georgia, Mississippi and Tennessee. University of Alabama Press, Tuscaloosa.

Zhang, Z., J. Zhu, Y. Chu, Z. Chen, S. Guo, and J. Xu. 2019. Correlation between microstructure and failure mechanism of *Hyriopsis cumingii* shell structure. Journal of Bionic Engineering 16:869–881.

Zieritz, A., J. I. Hoffman, W. Amos, and D. C. Aldridge. 2010. Phenotypic plasticity and genetic isolation-by-distance in the freshwater mussel *Unio pictorum* (Mollusca: Unionoida). Evolutionary Ecology 24:923–938.

Zuschin, M., and R. J. Stanton. 2001. Experimental measurement of shell strength and its taphonomic interpretation. Palaios 16:161–170.